

General Disclaimer

One or more of the Following Statements may affect this Document

- This document has been reproduced from the best copy furnished by the organizational source. It is being released in the interest of making available as much information as possible.
- This document may contain data, which exceeds the sheet parameters. It was furnished in this condition by the organizational source and is the best copy available.
- This document may contain tone-on-tone or color graphs, charts and/or pictures, which have been reproduced in black and white.
- This document is paginated as submitted by the original source.
- Portions of this document are not fully legible due to the historical nature of some of the material. However, it is the best reproduction available from the original submission.

NASA Technical Memorandum 86868

(NASA-TM-86868) THE REACTIONS OF COBALT,
IRON AND NICKEL IN SO-2 ATMOSPHERES:
SIMILARITIES AND DIFFERENCES (NASA) 13 p
HC A02/MF A01 CSCL 11F

N85-11217

Unclas
24256

G3/26

The Reactions of Cobalt, Iron and Nickel in SO₂ Atmospheres: Similarities and Differences

Nathan S. Jacobson
Lewis Research Center
Cleveland, Ohio

and

Wayne L. Worrell
University of Pennsylvania
Philadelphia, Pennsylvania



Prepared for
The Third International Conference on Transport
in Non-Stoichiometric Compounds
sponsored by Pennsylvania State University
University Park, Pennsylvania, June 11-15, 1984

NASA

THE REACTIONS OF COBALT, IRON AND NICKEL IN SO₂
ATMOSPHERES: SIMILARITIES AND DIFFERENCES

Nathan S. Jacobson
National Aeronautics and Space Administration
Lewis Research Center
Cleveland, Ohio 44135

and

Wayne L. Worrell
Department of Materials Science
University of Pennsylvania
Philadelphia, PA 19104

ABSTRACT

The reactions of cobalt, iron and nickel in SO₂ atmospheres are reviewed and compared. A mixed oxide-sulfide product layer is observed in all cases. Cobalt and nickel exhibit similar behavior. The observed rates are near the sulfidation rates, and the reaction rate is strongly influenced by the outward diffusion of metal through an interconnected sulfide network. A continuous interconnected sulfide is not observed in the oxide-sulfide scales formed on iron, and the reaction rates are more difficult to summarize. The differences and similarities among the three metals are explained in terms of the absence of scale-gas equilibrium and the ratio of the metal diffusivity in the corresponding oxide and sulfide.

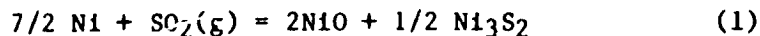
INTRODUCTION

In recent years, the reactions of cobalt, iron and nickel in SO₂ atmospheres have been studied extensively, and the understanding of the reaction mechanisms has significantly increased. In this paper, the scale growth mechanisms of these reactions are summarized, emphasizing the major similarities and differences. Our summary will consider only the SO₂ or SO₂-Ar atmospheres and studies below the lowest eutectic temperature in each system: 872°C for Co-Co₄S₃¹, 925°C for Fe-FeS-FeO², and 637°C for Ni₃S₂¹.

GENERAL THERMODYNAMIC AND KINETIC ASPECTS

A brief summary of the thermodynamic and kinetic aspects of these reactions is helpful before analyzing the mechanisms of scale growth. A thermodynamic stability diagram for each metal-sulfur-oxygen system is used to indicate which phases are stable

under the specified conditions of temperature, SO_2 and oxygen pressure³⁻⁵. For example, the stability diagram for the Ni-O-S system is shown in Fig. 1³. The reaction conditions considered in this analysis are temperatures below the eutectic temperature, SO_2 pressures between 0.1 and 1.0 atm, and an estimated oxygen impurity level of 1 PPM. Under these conditions, Fig. 1 indicates that the outer product scale would be nickel sulfate if scale-gas equilibrium were obtained. However it should be emphasized that when nickel is first exposed to SO_2 , the nickel activity is very high, and a mixed sulfide-oxide product scale can form according to reaction (1).



Thermodynamic calculations³ indicate that the nickel activity must be greater than 0.01 when the SO_2 pressure is between 0.25 and 1 atm. at 600°C for reaction (1) to proceed. Diagrams similar to Fig. 1 are also available for the Co-S-O⁴ and Fe-S-O⁵ systems. Under the conditions considered in this analysis, the outer product scale on cobalt should be either cobalt oxide and/or cobalt sulfate, while the equilibrium outer scale for iron is iron oxide. In all three cases, no metal sulfide should be observed at the scale-gas interface, because the sulfur activity in the SO_2 atmosphere is below that necessary for sulfide formation.

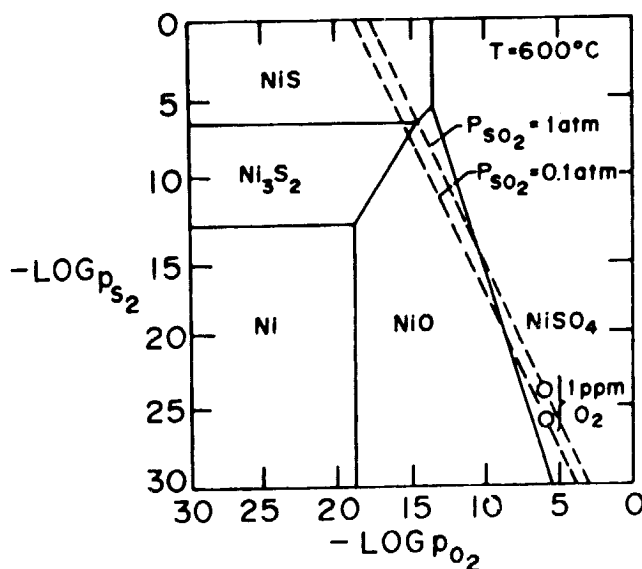
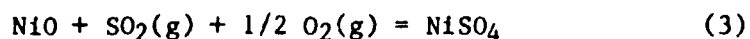
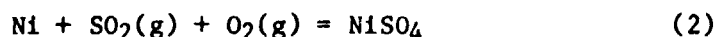


Fig. 1 Stability diagram for the Ni-S-O system at 600°C . The dotted lines are constant SO_2 pressure lines. The o points show the stable solid phase in the indicated SO_2 atmosphere, with an estimated O_2 impurity level of 1 PPM.

The observed presence of the metastable sulfide phase^{4,6} at the scale gas interface after extended reaction times is due to the combination of three factors. The first is that formation of sulfide-oxide product scales on metal surfaces with high metal activity is thermodynamically feasible, as discussed for reaction (1). The second factor is the large difficulty in the formation of sulfate in SO₂ atmospheres. For example, nickel sulfate is observed in several recent studies^{7,8} to form only by reaction of NiO with SO₃, and not by reactions (2) and/or (3).



Thus reaction (1) appears to be kinetically favored over reactions (2) and (3), because of a high activation-energy barrier in the direct formation of sulfate from solely SO₂ atmosphere. However, experimental studies using some of the newer surface-characterization techniques, e.g. in-situ Raman spectroscopy, are necessary to elucidate the kinetic barriers to sulfate formation. Once a sulfide-oxide product scale is formed, the third factor, metal diffusion through the scale becomes important. The high metal diffusivities in the sulfides shown in Table 1 could ensure that an abnormally high metal activity is maintained at the scale-gas interface and that reaction (1) continues to be favored over sulfate formation.

TABLE 1. Self-Diffusion Coefficients [$\text{cm}^2 - \text{sec}^{-1}$]

Cobalt, 750°C		Iron, 800°C		Nickel, 600°C	
CoS	$2.7 \times 10^{-8} (4,9)^a$	Fe _{0.9} S ^b	$1.3 \times 10^{-7} (10)$	Ni ₃ S ₂	$1.5 \times 10^{-7} (11)$
CoO ^b	$9.2 \times 10^{-11} (12)$	Fe _{0.9} O	$1.0 \times 10^{-7} (13)$	NiO	$3.0 \times 10^{-16} (14)$
		Fe ₃ O ₄	$3.3 \times 10^{-11} (13)$		

^a Reference from which value is obtained.

^b Single crystal samples, all others polycrystalline

The self-diffusion coefficients for cobalt, iron and nickel in the pertinent sulfides and oxides are compared in Table 1. For cobalt and iron, both single-crystal and polycrystalline data are listed, since grain boundary diffusion in their oxides or sulfides does not appear to be significant. Since only a polycrystalline value is available for Ni₃S₂, it is compared with a polycrystalline value for NiO. Table 1 clearly shows that metal diffusion through the sulfide is 10³ and 10⁹ times greater than through the oxide for cobalt and nickel, respectively. However, the iron diffusivity

is almost identical in FeS and FeO at 800°C. Because the product scales from the metal-SO₂ reactions contain both oxide and sulfide, the metal diffusivities in these phases must be considered in any kinetic analysis of the SO₂ reactions.

The parabolic-rate constants (k_p) for oxidation, sulfidation and SO₂ reaction for each of the three metals are summarized in Table 2. The values are presented in the units $\text{m moles gas}^2\text{-cm}^{-4}\text{-sec}^{-1}$ to enable a common basis of comparison between the three types of reaction. All the oxidation and sulfidation data are for oxygen and sulfur pressures of 1 atm, respectively, with the exception for nickel where the k_p is for oxidation at 0.1 atm. The k_p (SO₂) for nickel is for 0.25 atm, while the values for cobalt and iron are for 0.1 atm SO₂ pressure. The temperatures cited in Table 2 are those below the lowest eutectic temperature and having the largest amount of SO₂ reaction-rate data for each metal. The ratio of k_p (SO₂) to k_p (O₂) ranges from 10³ to 10⁷ for cobalt and nickel, respectively. However, the k_p (SO₂) for iron is close to the oxidation value.

TABLE 2. Parabolic-Rate Constants, [$\text{m moles}^2 - \text{cm}^4 - \text{sec}^{-1}$]

Metal	Oxidation	Sulfidation	SO ₂ Reaction
Cobalt, 750°C	$2.2 \times 10^{-7}(15)^a$	$3.9 \times 10^{-4}(16)$	$2.9 \times 10^{-4}(4)$
Iron, 800°C	$5.2 \times 10^{-5}(13)$	$8.2 \times 10^{-4}(9)$	$1.3 \times 10^{-5}(5)$
Nickel, 600°C	$3.0 \times 10^{-11}(17)$	$2.1 \times 10^{-4}(18)$	$1.4 \times 10^{-4}(6)$

^a Reference from which value is obtained.

SCALE GROWTH MECHANISMS IN SO₂ ATMOSPHERES

Cobalt

The reaction of cobalt in SO₂ atmosphere has been studied by numerous investigators^{4,19-22}. Product scales consist of a narrow band of cobalt sulfide adjacent to the metal and an outer two-phase oxide-sulfide layer (Fig. 2). Mechanisms of scale growth in 10% SO₂-Ar mixture at temperatures between 650 and 800°C have recently been reported⁴. An inner sulfide layer with an outer porous oxide layer form during the initial stages of reaction. Molecular SO₂ can penetrate the porous layer and react to form more oxide and sulfide.

When the oxide pores are filled with the sulfide-oxide reaction product, cobalt can diffuse rapidly through the sulfide phase to the scale-gas interface. At this point the outer two-phase sulfide-oxide scale (Fig. 2) begins to grow, and a parabolic rate law is observed at 700 and 750°C⁴. Cross-sectional micrographs

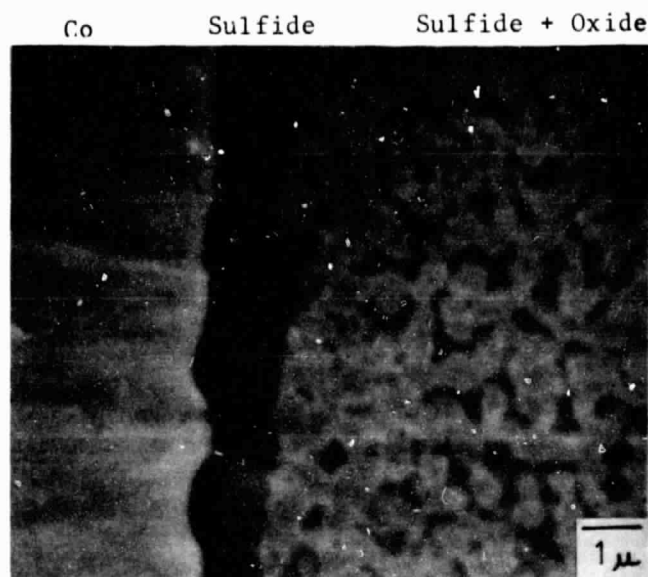


Fig. 2 Cross-sectional view of the product scale formed on cobalt after 2 hr at 750°C under 0.1 atm SO_2 ⁴. The sulfide is the dark phase. (Electron micrograph).

and electrical resistivity measurements of the product scale indicate that the sulfide phase is interconnected⁴. As shown in Table 1, the cobalt diffusivity in CoS is $\sim 10^3$ times greater than in CoO . This suggests that the interconnected sulfide phase acts as a rapid transport path for cobalt in the oxide matrix. The comparison of the cobalt diffusivities in CoS calculated from straight sulfidation and the SO_2 reactions shown in Table 3 confirms that cobalt diffusion through the sulfide phase is the primary mechanism establishing the scale-growth rate in SO_2 atmospheres. With increasing time the parabolic rates decrease, due to a change in the sulfide distribution in the outer sulfide-oxide scale⁴. The outer scale contains sulfide regions connected by narrow constricted sulfide channels in the oxide matrix, which results in restricted transport paths for cobalt.

IRON

The reaction of iron has been investigated in various SO_2 atmospheres including soley SO_2 ^{5,23,24}, $\text{N}_2\text{-O}_2\text{-SO}_2$ ²⁵, $\text{CO-CO}_2\text{-COS}$ ²⁵ and 10% $\text{SO}_2\text{-CO}_2$ ²⁶ gas mixtures. At low SO_2 pressures, the reaction has a linear rate with a clear flow-rate dependence, indicating that diffusion through a gaseous boundary layer at the scale-gas interface is rate limiting⁵. A typical cross-sectional view of the scale observed at 800°C in low pressure SO_2 environments is shown

TABLE 3. Calculated Cobalt and Nickel Diffusivities [$\text{cm}^2\text{-sec}^{-1}$] in CoS and Ni_3S_2 , respectively from Parabolic Ratio Constants for Sulfidation and SO_2 Reactions.

Sulfide, Temp.	D_M , Sulfidation ^a	D_M , SO_2 Reaction ^b
CoS, 700°C	9.8×10^{-9}	2.2×10^{-8} (0.1 atm SO_2)
CoS, 750°C	2.7×10^{-8}	4.2×10^{-8} (0.1 atm SO_2)
Ni_3S_2 , 600°C	1.5×10^{-7}	0.7×10^{-7} (0.25 atm SO_2)
Ni_3S_2 , 600°C	1.5×10^{-7}	2.7×10^{-7} (1 atm SO_2)

^a Sulfidation data from references 4 and 9 for CoS and reference 11 for Ni_3S_2 .

^b SO_2 -reaction data from reference 4 for CoS and reference 6 for Ni_3S_2 .

in Fig. 3. Although the scale consists of sulfide and oxide, its morphology is very different than that observed with cobalt and nickel. In Fig. 3, a finely dispersed FeO-FeS duplex layer is observed adjacent to the iron instead of the narrow, continuous sulfide layer observed with cobalt and nickel. A lamellar FeO-FeS layer is also observed on top of the inner duplex layer. The observed morphology has been postulated to result from a SO_2 reaction where the formation of FeO increases the sulfur activity to form FeS which in turn increases the oxygen activity to form FeO^5 .

At higher SO_2 pressures and extended times, parabolic reaction kinetics have been reported^{5,23,24}. The scale morphologies are very complicated, and quantitative interpretation of the observed parabolic rates is not possible. The absence of an interconnected sulfide network in the product scale as observed with cobalt and nickel is presumably related to the similar values for the iron diffusivity in FeS and FeO shown in Table 1. In the oxide-sulfide product scale on iron, an interconnected FeS network in FeO would not enhance the transport of iron to the scale-gas interface. Thus the observed parabolic-rate constants for iron- SO_2 reactions are similar to those observed in the oxidation of iron^{5,23}. For example, the value shown in Table 2 for the iron- SO_2 reaction is slightly less than that shown for iron oxidation, while the values for the SO_2 reactions with cobalt and nickel are 10^3 to 10^7 faster than their respective oxidation rates.

ORIGINAL PAGE IS
OF POOR QUALITY

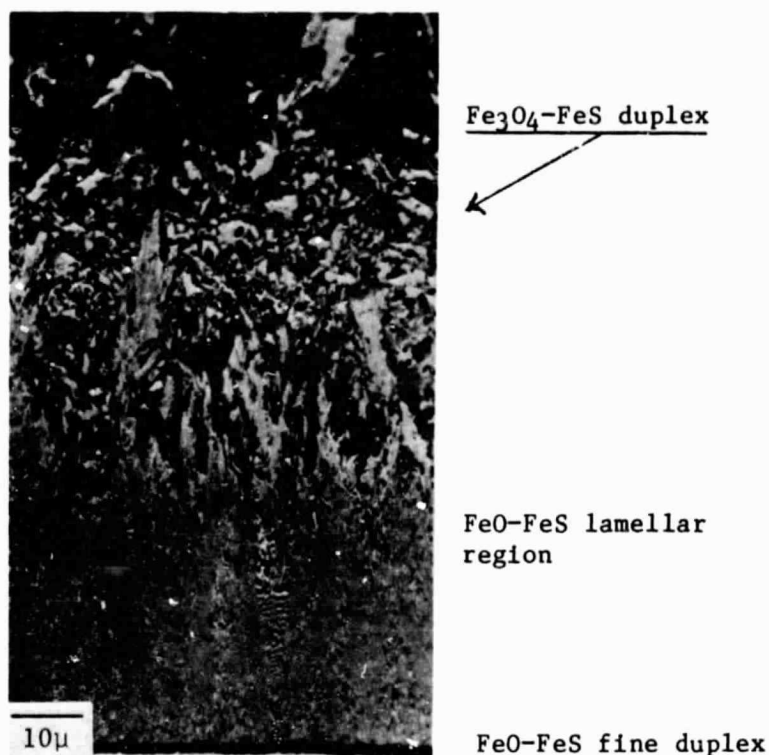


Fig. 3 Cross-sectional view of the product scale formed on iron at 800°C under low SO₂ pressures (~0.1 atm)⁵. The sulfide phase is the light region (optical micrograph).

NICKEL

The reaction of nickel in SO₂ atmosphere has been extensively investigated^{6,27-32}. The reaction mechanism^{6,27,28,31} in solely SO₂ atmospheres and at temperatures below 637°C (the Ni-Ni₃S₂ eutectic temperature) is summarized here. During the early stages of reaction, a porous NiO layer forms on the nickel while the sulfur from the dissociation of SO₂ diffuses through the nickel grain boundaries to form an inner layer of Ni₃S₂⁶. Eventually the pores are filled with the sulfate-oxide product of reaction (1), and nickel can diffuse through the sulfide to the scale-gas interface. After this initial stage, the outer two-phase (NiO-Ni₃S₂) layer begins to grow and parabolic, diffusion controlled kinetics are observed. Inert markers are located between the inner Ni₃S₂ layer and the outer two-phase layer²⁷⁻²⁹, confirming that the inner layer grows by inward sulfur diffusion and the outer two-phase layer grows by outward nickel diffusion. The thickness of the inner

ORIGINAL PAGE IS
OF POOR QUALITY

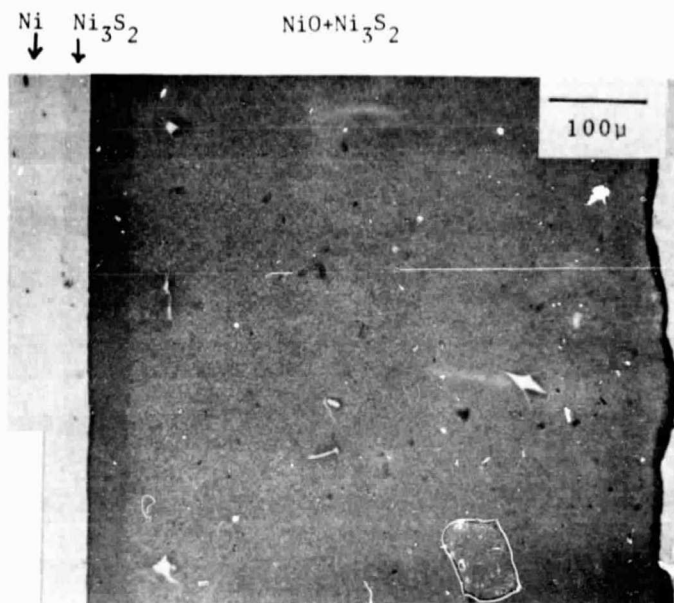


Fig. 4 Cross-sectional view of the scale formed on nickel after 44 min at 603°C under 1 atm SO₂⁶. The sulfide is the light phase (optical micrograph).

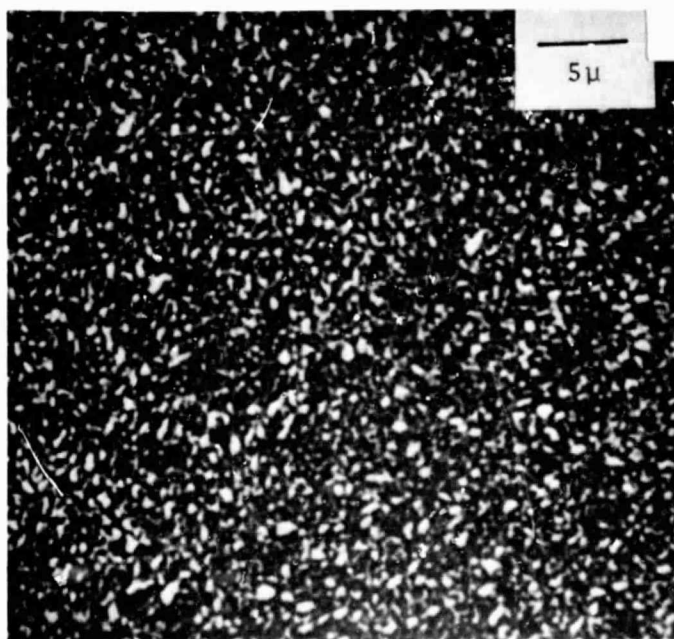


Fig. 5 Higher magnification of the outer two-phase scale shown in Fig. 4⁶. The Ni₃S₂ (light regions) is fairly uniformly distributed in NiO.

Ni_3S_2 layer at 600°C is $\sim 30\mu$ (Fig. 4), while the inner sulfide layer form on cobalt at 750°C (Fig. 2) is only $\sim 1\mu$ thick. This comparison indicates that the grain-boundary diffusivity of sulfur is significantly higher in nickel than in cobalt.

Figure 5 is a highly magnified picture of the outer two-phase region of the product scale shown in Fig. 4. The lighter areas are the Ni_3S_2 phase, which is rather evenly distributed in the darker oxide matrix. Resistivity measurements indicate that the Ni_3S_2 is interconnected throughout the outer two-phase layer⁶. The nickel diffusivity in Ni_3S_2 is about 10^9 times greater than that in NiO at 600°C (see Table 1), and the Ni_3S_2 phase provides a rapid transport path for nickel diffusion through the outer two-phase scale. Calculated values of the nickel diffusivity from the parabolic rate constants of nickel- SO_2 reactions⁶ are shown in Table 3. The agreement between these calculated values and that obtained from sulfidation experiments confirms that nickel diffusion through interconnected Ni_3S_2 is the primary mechanism controlling the growth rate of the outer, two-phase scale. Thus the parabolic growth rates observed for the nickel- SO_2 and the cobalt- SO_2 reactions are controlled by similar mechanisms.

SUMMARY AND CONCLUSIONS

The reactions of cobalt, iron and nickel in SO_2 atmospheres have been compared. In all three metal- SO_2 reactions, a metastable sulfide phase is observed at the scale-gas interface. The presence of the sulfide phase is due to three factors: formation of sulfide from SO_2 is thermodynamically feasible at high metal activities, the large difficulty in the formation of sulfate from SO_2 , and rapid metal diffusion through the two-phase product scales maintains a high metal activity at the scale-gas interface.

Cobalt and nickel exhibit similar behavior in that both form an inner thin sulfide layer adjacent to the metal and an outer two-phase layer consisting of an interconnected sulfide phase in an oxide matrix. The metal diffusivity is much greater in the sulfide than in the oxide, and the interconnected sulfide provides a rapid transport path for metal diffusion through the outer two-phase scale. The observed parabolic-rate constants for the SO_2 reactions are 10^3 to 10^7 times greater than those observed for oxidation.

The reaction of iron in SO_2 atmosphere is more complex, because of the influence of gas transport and the similar values of the iron diffusivity in FeS and FeO . The morphology of the scales formed on iron is very complicated, and quantitative interpretation of the parabolic kinetics is not possible. However, the observed parabolic rates are similar to those observed in the oxidation of iron.

ACKNOWLEDGEMENTS

The support of the NSF Materials Research Program under Grant No. DMR-7923647 at the University of Pennsylvania for our investigations of the nickel-SO₂ and cobalt-SO₂ reactions is gratefully acknowledged. The authors also thank Dr. Ajay Misra of NASA Lewis Research Center for helpful discussions.

REFERENCES

1. T. Rosenqvist, *J.I.S.I.*, 176, 37 (1954).
2. D. C. Hilty and W. Crofts, *Trans. AIME*, 194, 1307 (1952).
3. N. S. Jacobson and W. L. Worrell in Proceedings of the Symposium on High Temperature Materials Chemistry II, Electrochemical Society, Inc., Pennington, 1983, pp. 217-223.
4. N. S. Jacobson and W. L. Worrell, *J. Electrochem. Soc.* 131, 1182 (1984).
5. T. Flatley and N. Birks, *J.I.S.I.*, 209, 523 (1971).
6. K. L. Luthra and W. L. Worrell, *Met. Trans.* 9A, 1055 (1978).
7. W. L. Worrell and B. Ghosal in Proceedings JMIS-3, High Temperature Corrosion, *Trans. JIM, Suppl.*, 1983, pp. 419-426.
8. V. Guerra-Brady and W. L. Worrell, to be published.
9. S. Mrowec and T. Werber, *Chemia Analityczna* 7, 605 (1962).
10. R. H. Condit, R. R. Hobbins, and C. E. Birchenall, *Oxide Met.* 8, 409 (1974).
11. B. D. Bastow and G. C. Wood, *Oxide Met.* 9, 473 (1975).
12. R. E. Carter and F. D. Richardson, *Trans. AIME* 200, 1244 (1954).
13. L. Himmel, R. F. Mehl, and C. E. Birchenall, *Trans. AIME*, 197, 827 (1953).
14. K. Fueki and J. B. Wagner, *J. Electrochem. Soc.* 112, 384 (1965).
15. H. S. Hsu and G. J. Yurek, *Oxid. Met.* 17, 55 (1982).
16. S. Mrowec and T. Werber, *Phys. Met. Metallogr.* (Engl. Transl.) 8, No. 3, 452 (1959).
17. E. A. Gulbransen and K. F. Andrew, *J. Electrochem. Soc.* 101, 128 (1954).
18. L. Czerski, S. Mrowec, and T. Werber, *J. Electrochem. Soc.* 109, 273 (1962).
19. P. Singh and N. Birks, *Oxid. Met.* 12, 23 (1978).
20. F. Gesmundo and C. deAsmundis in "Behavior of High Temperature Alloys in Aggressive Environments; Proceedings of the International Conference, Petten, The Netherlands, 15-18 October, 1979" pp 435-447, Metals Society, London (1980).
21. K. Holthe and P. Kofstad, *Corros. Sci.* 20, 919 (1980).
22. B. Gillot and D. Garnier, *Ann. Chim. Fr.* 5, 483 (1980).
23. B. Chatterjee and A. D. Dowell, *Corros. Sci.* 15, 637 (1975).
24. F. Gesmundo, C. deAsmundis, S. Merk, and C. Bottino, *Werkstoffe und Korrosion*, 30, 179 (1979).
25. A. Rahmel, *Corros. Sci.*, 13, 125 (1973).

26. F. C. Yang and D. P. Whittle in Proceedings of the Symposium on Corrosion in Fossil Fuel Systems, The Electrochemical Society, Pennington, 1983, pp 111-129.
27. C. B. Alcock, M. G. Hocking, and S. Zador, *Corros. Sci.* 9, 111 (1969).
28. M. R. Wootton and N. Birks, *Corros. Sci.* 12, 829, (1972).
29. P. Kofstad and G. F. Axelson, *Oxid. Met.* 12, 503 (1978).
30. K. L. Luthra and W. L. Worrell, *Met. Trans.* 10A, 621 (1979).
31. M. Seierstein and P. Kofstad, *Corros. Sci.* 12, 487 (1982).
32. B. Haflan and P. Kofstad, *Corros. Sci.* 23, 1333 (1983).